available at www.sciencedirect.com

ScienceDirect

journal homepage: www.elsevier.com/locate/agrformet

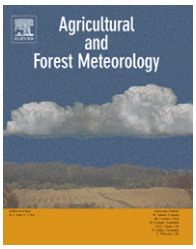

Multiple site tower flux and remote sensing comparisons of tropical forest dynamics in Monsoon Asia

A.R. Huete [a,c,*], N. Restrepo-Coupe [b], P. Ratana [d], K. Didan [a], S.R. Saleska [b,c], K. Ichii [e], S. Panuthai [f], M. Gamo [g]

[a] Department of Soil, Water & Environmental Science, University of Arizona, Tucson, AZ 85721, USA
[b] Department of Ecology and Evolutionary Biology, University of Arizona, Tucson, AZ 85721, USA
[c] Institute for the Study of Planet Earth, University of Arizona, Tucson, AZ 85721, USA
[d] Department of Geotechnology, Khon Kaen University, Khon Kaen, Thailand
[e] San Jose State University and Ecosystem Science and Technology Branch, NASA Ames Research Center, Mail Stop 242-4, Moffett Field, CA 94035, USA
[f] National Park, Wildlife and Plant Conservation Department, Chatuchak, Bangkok 10900, Thailand
[g] National Institute of Advanced Industrial Science and Technology (AIST), Tsukuba, Ibaraki 305-8569, Japan

ARTICLE INFO

Article history:
Received 6 June 2007
Received in revised form
25 December 2007
Accepted 18 January 2008

Keywords:
AsiaFlux
Remote sensing
MODIS E_{VI}
Tropical forests
Phenology

ABSTRACT

The spatial and temporal dynamics of tropical forest functioning are poorly understood, partly attributed to a weak seasonality and high tree species diversity at the landscape scale. Recent neotropical rainforest studies with local tower flux measurements have revealed strong seasonal carbon fluxes that follow the availability of sunlight in intact forests, while in areas of forest disturbance, carbon fluxes more closely tracked seasonal water availability. These studies also showed a strong seasonal correspondence of satellite measures of greenness, using the Enhanced Vegetation Index (E_{VI}) with ecosystem carbon fluxes in both intact and disturbed forests, which may enable larger scale extension of tower flux measurements.

In this study, we investigated the seasonal patterns and relationships of local site tower flux measures of gross primary productivity (P_g) with independent Moderate Resolution Imaging Spectroradiometer (MODIS) satellite greenness measures across three Monsoon Asia tropical forest types, encompassing drought-deciduous, dry evergreen, and humid evergreen secondary tropical forests. In contrast to neotropical forests, the tropical forests of Monsoon Asia are more extensively degraded and heterogeneous due to intense land use pressures, and therefore, may exhibit unique seasonal patterns of ecosystem fluxes that are more likely water-limited and drought-susceptible.

Our results show significant phenologic variability and response to moisture and light controls across the three tropical forest sites and at the regional scale. The drier tropical forests were primarily water-limited, while the wet evergreen secondary forest showed a slight positive trend with light availability. Satellite E_{VI} greenness observations were generally synchronized and linearly related with seasonal and inter-annual tower flux P_g measurements at the multiple sites and provided better opportunities for tower extension of carbon fluxes than other satellite products, such as the MODIS P_g product. Satellite E_{VI}-derived P_g images revealed strong seasonal variations in photosynthetic activity throughout the Monsoon Asia tropical region.

* *Corresponding author at*: Department of Soil, Water & Environmental Science, University of Arizona, Tucson, AZ 85721, USA. Tel.: +1 520 621 3228.
E-mail address: ahuete@ag.arizona.edu (A.R. Huete).
0168-1923/$ – see front matter
doi:10.1016/j.agrformet.2008.01.012

1. Introduction

Tropical forests comprise a major and critical component of the global Earth system through their role in climate and hydrologic and biogeochemical cycling, and as a principal reservoir of the planet's biological diversity. Tropical forest ecosystems also have social, cultural and economic significance as sources of important renewable and non-renewable resources (Defries et al., 1995; Achard et al., 2002). Despite their importance, the mechanisms, interactions, and impact of environmental and human factors on tropical forest functioning remain poorly understood. Knowledge of tropical forest temporal dynamics and spatial heterogeneities at multiple scales is necessary to understand how of these ecosystems may respond to or adapt to global change and human interactions (Schurr et al., 2006; Mahli et al., 1998; Skole and Tucker, 1993).

Southeast Asia has some of the highest carbon density regions in the world, however, tropical forest degradation is prominent and deforestation rates are among the highest on the planet, induced by the region's large and growing human population and the increasing exploitation of forest resources (Page et al., 2002; Tian et al., 2003). An understanding of the impact of climate variability and human factors on Monsoon Asia tropical forest functioning and sustainability becomes particularly crucial with important consequences to carbon balance and emissions, fire susceptibility, and resulting air quality and public health (Achard et al., 2002).

At the landscape level, many climate and productivity models characterize tropical evergreen rainforests as lacking seasonal variation in biophysical plant properties such as greenness, leaf area index (L_{ai}), fraction of photosynthetically active radiation absorbed (f_{par}), and albedo (Lean and Rowntree, 1993; Sellers et al., 1995). Much of what is known about tropical ecosystem dynamics and climate–vegetation interactions comes from coarse resolution, high temporal frequency satellite measurements, such as the NOAA-Advanced Very High Resolution Radiometer (AVHRR) time series data, which also have characterized the phenology of tropical evergreen forests as seasonally constant (Justice et al., 1985; Running et al., 1994; Defries et al., 1995; Achard and Estreguil, 1995; Skole and Qi, 2001; Eva et al., 2004). Phenologic variations, a characteristic property of ecosystem functioning and predictor of ecosystem processes, are important to resolve, as they depict a canopies' integrated response to environmental change and influence local biogeochemical processes, including nutrient dynamics, photosynthesis, water cycling, soil moisture depletion, and canopy physiology (Reich and Borchert, 1984).

On the other hand, plot-level and local-scale studies have shown distinct seasonal changes in tropical forest canopy characteristics, including flushing and exchange of new leaves, periods of decreased foliage density, leaf aging, senescence, and litterfall (Frankie et al., 1974; Wright and Schaik, 1994). Roberts et al. (1998) found seasonal variations in canopy optical properties associated with leaf aging, epiphyll activity in the wet season, and leaf flushing in the dry season in a dense caatinga tropical forest near Manaus in central Amazon. Wright and Schaik (1994) found leaf flushing and flower production at sites across eight different rainforests, including sites in Borneo and East Java, to closely coincide with dry season peaks in incident photosynthetic active radiation (I_{par}). Carswell et al. (2002) and Asner et al. (2004) measured increases in plot-level leaf area index (L_{ai}) in the dry season at two eastern Amazon evergreen rainforest sites.

More recent, eddy flux tower measurements have also shown seasonal patterns in canopy photosynthesis that follow the availability of sunlight in neotropical evergreen forests in the Amazon (Carswell et al., 2002; Saleska et al., 2003; da Rocha et al., 2004; Goulden et al., 2004). Seasonal peaks in evapotranspiration (E_T) have been measured in the late dry season in tropical evergreen forests in northern Thailand and in Amazon (Shuttleworth, 1988; Tanaka et al., 2004; da Rocha et al., 2004). These forests showed little evidence of moisture stress during the dry season with tree roots maintaining access to deep soil moisture layers (Nepstad et al., 1994; Tanaka et al., 2003; da Rocha et al., 2004).

One reason for the ambiguity and lack of knowledge of topical forest seasonality at the landscape scale is their complexity, where a highly diverse tree species population can result in a wide variety of phenology responses to the same or common environmental factors, such as rainfall, temperature, and photoperiod (Wright and Schaik, 1994; Reich et al., 2004; Prior et al., 2004; Kushwaha and Singh, 2005). Several constraints inherent in coarse resolution satellite data may also contribute to the difficulties in detecting temporal and spatial variability in tropical forest phenology, including poor spatial resolution (>4 km), cloud contamination, sensitivity to seasonally variable atmosphere water vapor and aerosol conditions, limited spectral content, and low optical depth of penetration through densely vegetated canopies (Goward et al., 1991; Skole and Qi, 2001). Kobayashi and Dye (2005) found cloud and aerosol seasonal influences in AVHRR normalized difference vegetation index (N_{DVI}) data to mask the apparent weak tropical forest seasonal signal from the Amazon.

Finer resolution satellite data (e.g., Landsat) offer more accurate monitoring and discrimination of tropical forests and disturbance events, such as deforestation and fire (Cihlar et al., 1997; Defries et al., 1995; Mayaux and Lambin, 1997; Vieira et al., 2003; Kalacska et al., 2005). However, it is difficult to obtain sufficient cloud-free images at the frequencies needed to define accurate phenology trends. Furthermore, saturation of the N_{DVI} in tropical forests has been noted in both fine and coarse resolution satellite data, resulting in a lack of sensitivity to detect seasonality in forest canopy biophysical and biochemical properties, discriminate primary from regenerating forests, and assess phenology characteristics, such as leaf age (Sader et al., 1989; Skole and Qi, 2001; Huete et al., 2002; Xiao et al., 2005; Zhang et al., 2005).

Some of the more recent and advanced moderate resolution satellite sensors, such as SPOT VEGETATION (VGT) and the Moderate Resolution Imaging Spectroradiometer (MODIS) have better sensor capabilities for tropical ecosystem studies with improved calibration and atmosphere correction, narrower spectral bands, and finer resolution observations (250–1000 m) that facilitate cloud-filtering and noise removal (Justice et al., 1998). Distinct local- and region-wide phenology patterns have been observed in Amazon forests with MODIS-derived leaf area index (L_{ai}) and MODIS and SPOT-VGT

enhanced vegetation index (E_{VI}, an index of canopy photosynthetic capacity) (Huete et al., 2006; Xiao et al., 2006; Myneni et al., 2007). Furthermore, a strong seasonal correspondence of satellite E_{VI} values with tower flux measurements of gross primary productivity (P_g) was found over intact Amazon rainforests that followed the availability of sunlight (Xiao et al., 2005; Huete et al., 2006). In areas of tropical forest conversion to pasture and agriculture, a reversal in satellite greenness phenology and tower P_g seasonal fluxes occurred, with dry season declines in photosynthetic capacity, due to the replacement of deep-rooted forest trees with shallower rooting systems that became drought prone to extended dry periods (Saleska et al., 2003; Huete et al., 2006).

Vegetation with root fractions occupying shallower soil layers, as in younger secondary forests, are increasingly susceptible to water stress and show phenologies more controlled by soil moisture (Tanaka et al., 2004; Huete et al., 2008). Curran et al. (2004) found that intact rainforests in the Kalimantan rainforests of Borneo were able to survive ENSO events, however, disturbed areas became drought-susceptible, triggering widespread fires and a drastic reduction in the regenerative capacity of the rainforests. Saleska et al. (2007) showed the intact rainforests in the Amazon were highly resilient to periods of water shortage, as in the 2005 intense drought, and were more productive due to increased sunlight. Moisture and sunlight controls on tropical forest seasonal dynamics and productivity vary with climatic and human drivers, as well as ecological conditions. At regional scales, a complex mosaic of vegetation function and phenology patterns may be expected as a result of forest structural variations, soil properties, topography effects, land use activities, forest disturbance and conversion, and climate variability (e.g., duration and intensity of the dry season) (Asner et al., 2004; Keller et al., 2004).

An accurate representation of the seasonal and spatial dynamics of tropical forest functioning and phenology is prerequisite to drive ecosystem productivity models and predict future inter-annual trends and changes resulting from climate change and land use impacts (Nemani et al., 2003; Viña and Henebry, 2005; White et al., 2005). The use of tower flux measurements in different vegetation types can serve to calibrate spatially extensive satellite data to improve predictions and modeling of regional carbon fluxes. In this study we compared simultaneously acquired tower flux and satellite measurements of vegetation dynamics across three different Monsoon Asia tropical forest types. Our objectives were to analyze the spatial and temporal variability in tropical forest functioning and phenology and assess the potential coupling of multiple tower sites, each with limited and fairly narrow spatial scales, with satellite measurements for larger scale extension of carbon fluxes.

2. Study sites and methods

2.1. Study sites

We analyzed eddy flux tower datasets of carbon and radiation dynamics across three different tropical forest types that are part of the AsiaFlux network (www.asiaflux.net), including a monsoonal drought-deciduous forest, a monsoonal dry evergreen forest, and a humid evergreen tropical forest (Fig. 1). Regional differences in tropical forest types can be attributed to climate regime and soil influences with dry monsoonal forests occurring in areas with annual precipitation below 2000 mm and with a distinct dry season of 2–6 months (Ishida et al., 2006). The tropical drought-deciduous forests lose their leaves under dry conditions, while the tropical evergreen trees develop deeper roots to maintain leaves and transpiration through dry conditions (Canadell et al., 1996).

The drought-deciduous tropical forest tower site is located within the MaeKlong Watershed Research Station in Kanchanaburi Province, about 250 km northwest of Bangkok, Thailand (Table 1). This secondary forest of 30+ years is a mixed (~50%) deciduous canopy, dominated by *Shorea siamensis*, *Vitex peduncularis*, and *Xylia xylocarpa* tree species, forming a multilayer canopy of approximately 20–30 m height and total L_{ai} of 2–3. Mean annual rainfall is 1650 mm with a dry season from November to March. The drought-avoiding deciduous species lose their leaves during the latter half of the dry season (January–March) and there is a flushing of new leaves in April, following the onset of rainfall (Ishida et al., 2006). The soils are classified as Kandiustalfs and are relatively rich in nutrients (Rundel and Boonpragob, 1995).

The evergreen dry tropical forest tower site is located within the Sakaerat Environmental Research Station in Nakhon Ratchasima Province, about 180 km northeast of Bangkok, Thailand (Table 1). The research station is located on a table mountain, within the Korat sandstone plateau, ranging in elevation from 650 to 250 m and dissected by a branch of the Mekong River. The most dominant tree species, *Hopea ferrea Lanessan* is in the Dipterocarpaceae family and makes up the top canopy layer (Pitman, 1996). Mean annual rainfall is 1240 mm (Ishida et al., 2006) with a dry season similar to that of the MaeKlong Station (November–March), but there is no leafless period in the drought-tolerant evergreen species and overall leaf life span may reach 2 years. The soils are classified as Tropustults, and are predominantly shallow, sandy loam texture, acidic, and nutrient poor (Pitman, 1996; Rundel and Boonpragob, 1995).

The humid evergreen tropical rainforest tower site is located within Bukit Soeharto Education Forest of Mulawarman University within the Bukit Soeharto National Park on the east coast of East Kalimantan, Indonesia. Forest area has decreased rapidly on the island of Borneo, which was once almost completely covered by tropical rainforest. This area was granted protection status by the government of Indonesia in 1978 but has experienced large-scale forest fires during the exceptionally dry years in 1982–1983 and 1997–1998, linked to particularly strong El Niño events. The present young successional forest stands consist of semi-natural dipterocarp forest, together with degraded forest and plantation forest stands. The dominant species, *Macaranga gigantea* and related species, have canopy heights of about 10–20 m, total L_{ai} of 3, and have regenerated 3–6 years (1998 fire) during the 4 years of data analyzed here. The coastal lowlands in the central and southern parts of East Kalimantan have a seasonally weak drier period from July–August to October, during which precipitation is 80–150 mm/month, and are at times subject to periodic droughts.

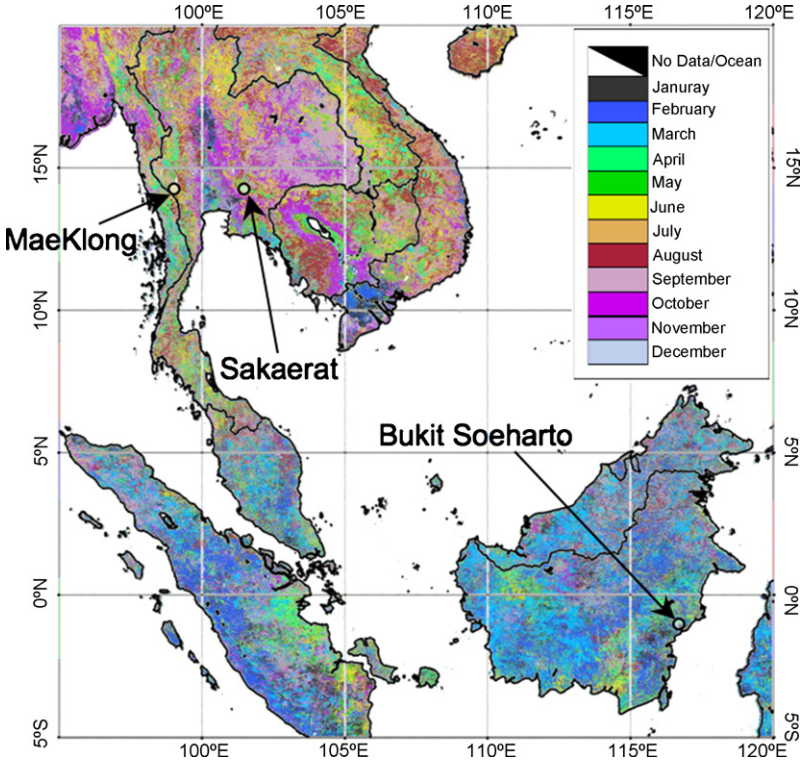

Fig. 1 – Location of three tropical forest study areas overlain onto a MODIS E_{VI} satellite phenology depiction of month of peak vegetation activity.

2.2. *Methods*

Tower flux estimates of canopy–atmosphere CO_2 gas exchange, aggregated at half hour intervals, were obtained by eddy-covariance method (Gamo et al., 2005). Three similar closed-path eddy-covariance systems are installed at 45, 42, and 18.4 m heights at Sakaerat, MaeKlong, and Bukit Soeharto sites, respectively. The standard eddy flux system consists of a 3-axis sonic anemometer (Wind Master, Gill, T-540, Kaijo) and a closed-path CO_2/H_2O analyzer (LI-6262, LI-COR) with a sampling rate of 4 Hz at the Sakaerta and Bukit Soeharto sites and 10 Hz at MaeKlong site. All flux and meteorological datasets were quality checked and outliers and measurements made during rainy periods removed. Comparisons between different instruments were also used to discard faulty data.

The gross canopy photosynthetic flux is calculated as

$$P_g = -(N_e - R_{eco}) \quad (1)$$

where P_g is gross ecosystem production, N_e is net ecosystem exchange of CO_2 between the forest and the atmosphere (with

Table 1 – Description and location of the three tropical forest types analyzed

	MaeKlong Watershed Research Station, Thailand	Sakaerat Environmental Research Center, Thailand	Bukit Soeharto, East Kalimantan, Indonesia
Latitude/longitude	14°34.57′N 98°50.62′E	14°29.6′N 101°55.32′E	0°51.68′S 117°2.68′E
Elevation	160 m	535 m	20 m
Vegetation type	Tropical seasonal broadleaf deciduous forest (*Shorea siamensis, Vitex peduncularis, Xylia xylocarpa*), >30 years old	Tropical dry evergreen broadleaf forest (*Hopea ferrea Pierre*)	Regenerating tropical rainforest (*Macaranga gigantea*) (since 1998)
Canopy height/L_{ai}	20–30 m/2–3	35 m/3.5–4	>10 m/3
Mean annual temperature and rainfall	27.5 °C 1650 mm	26.2 °C 1240 mm	28.0 °C 2002 mm
Soils	Kandiustalfs, clay loam texture	Shallow Stony Ultisols, sandy loam (acidic)	Typic Paleudults (US Soil Taxonomy)

fluxes to the atmosphere defined as positive) and R_{eco} is ecosystem respiration. Note that Eq. (1) defines P_g as a positive number. N_e is calculated as the sum of CO_2 eddy flux at the top of the tower (F_c) and the rate of change in CO_2 in the canopy air space. Analysis of the relation between N_e and atmospheric turbulence (as indicated by friction velocity, u^*) suggested that nighttime N_e likely underestimates the true biotic respiration flux during periods of low turbulence (Goulden et al., 1996; Saleska et al., 2003). We, therefore, excluded N_e measurements taken when u^* fell below the threshold at which underestimation became evident. Our analysis indicated u^* thresholds of 0.4 (at Sakaerat), 0.2 (at MaeKlong), and 0.1 m s^{-1} (at Bukit Soeharto).

R_{eco} was calculated as the average of nighttime N_e over a 5-day moving window. If the 5-day window was not sufficient, after removal of data by u^* filtering, to give at least 10 h of nighttime data, we extended the length of the window (up to 31 days) until at least 10 h of valid nighttime data were included.

We observed no significant correlation between hourly nighttime N_e measurements and nighttime air temperature at any of the 3 sites (probably because nighttime temperature variation was small), so daytime R_{eco} was assumed equal to nighttime R_{eco}. This approach is similar to that taken in the Amazon (Saleska et al., 2003). Because of the temperature sensitivity of R_{eco} and warmer daytime temperature, this assumption probably slightly underestimates daytime R_{eco} (and hence P_g), but it is unlikely to affect the seasonal patterns.

In order to avoid bias in monthly P_g which would likely result from simply averaging valid hourly P_g data to monthly levels (because of a fair-weather bias in valid data), we used an unbiased look-up table approach to fill missing P_g data before averaging. Missing P_g was modeled with a look-up-table (LUT) filled with mean observed P_g as a function of both incident photosynthetically active radiation (I_{par}) (bin-width of 200 μmol m^{-2} s^{-1}) and hour-of-day (2-h wide bins). The P_g entries in the LUT were calculated from a moving window of 11 days (extended to longer periods, up to 31 days, if necessary to include at least 16 h of valid daytime data). Hour-of-day bins capture clear differences between morning and afternoon light-use-efficiency, seen also in other tropical forests (e.g., Goulden et al., 2004; Hutyra et al., 2007), and the moving window captures differences due to changes in soil moisture or seasonal patterns. Gaps inside the LUT were filled using a linear interpolation and the nearest neighbor method was used when extrapolation was required. Finally, we averaged the valid observed and filled hourly P_g values to generate monthly values.

Volumetric soil moisture data were measured at 30 min temporal resolution with Time Domain Reflectometry (TDR) sensors at 10 cm soil depth. I_{par} at the tower sites was measured at 30 min resolution with quantum sensors. We generated monthly values from daily averages of soil water content and daytime averages of I_{par}. Monthly rainfall data was obtained from the Tropical Rainfall Measuring Mission (TRMM 3B43-v6) satellite time series at 0.25° × 0.25° resolution (NASA, 2007). Monthly means of hourly downward surface solar radiation data at one degree spatial resolution, generated from the Terra Clouds and the Earth's Radiant Energy System (CERES) and Geostationary Operational Environmental Satellite 8 (GOES-8) instruments, was obtained from the Langley Atmospheric Sciences Data Center (eosweb.larc.nasa.gov/PRODOCS/ceres/table_ceres.php).

Satellite-derived phenology over the local tower sites and Southeast Asia region was derived with 4 years (2001–2004) of MODIS measures of 'greenness', using the MOD13A2 Enhanced Vegetation Index (E_{VI}) at 1 km spatial resolution and MOD13Q1 at 250 m resolution. The MODIS vegetation index (V_I) products are composited to 16-day intervals using strict quality assurance (QA) criteria to remove residual cloud and aerosol contamination. The 16-day composites were aggregated to monthly time steps and only the good QA pixels within a 3 × 3 pixel window were averaged for comparison with the tower flux measurements. A 4-year average seasonal profile was also computed for regional phenology analysis and an image depicting per pixel peak month in annual E_{VI} values was derived (Fig. 1). The E_{VI} is an optimized combination of reflectances in the red and near-infrared (NIR) bands, based on 1st-order Beer's law application of canopy radiative transfer, that extends sensitivity in high biomass canopies and removes greenness biases from differences in soil background,

$$E_{VI} = 2.5\frac{\rho_N - \rho_R}{L + \rho_N + C_1\rho_R - C_2\rho_B}, \quad (2)$$

where E_{VI} is the enhanced vegetation index, $\rho_{N,R,B}$ are reflectances in the NIR, red, and blue bands, respectively; L is the canopy background adjustment factor; and C_1 and C_2 are the aerosol resistance weights. The coefficients of the MODIS E_{VI} equation are $L = 1$; $C_1 = 6$ and $C_2 = 7.5$ (Huete et al., 2002).

We also examined the seasonal vegetation patterns of the tropical forest sites with the MODIS-derived fraction of photosynthetically active radiation absorbed (f_{par}, MOD15), gross primary production (P_g, MOD17), and N_{DVI} (MOD13Q1, MOD13A2) products obtained from the Oak Ridge National Laboratory (ORNL) MODIS subsets (http://www.daac.ornl.gov/). The MODIS P_g product is based on a light-use efficiency model that uses the MODIS f_{par} product, and large spatial scale meteorological solar radiation, vapor pressure, and temperature from the NASA Data Assimilation Office as inputs. For each product, we used the average of good QA pixels within a 3 km × 3 km window centered at the flux tower and generated an average seasonal profile from the 4 years of data.

3. Results

3.1. *MaeKlong drought-deciduous tropical dry forest*

Seasonal and inter-annual trends in tower flux P_g and satellite E_{VI} greenness measurements were strongly synchronized with each other across the 4 years at the MaeKlong drought-deciduous tropical forest site (Fig. 2). There is a distinct phenology in this mixed drought-deciduous, water-limited ecosystem with leaf flushing of new leaves commencing with the onset of the rainy season in May, followed by peak activity in the middle of the wet season (June–August), and decreasing vegetation activity (photosynthesis and greenness) through the second half of the wet season (September–November). There is a rapid loss of leaves in 2 months into the dry season

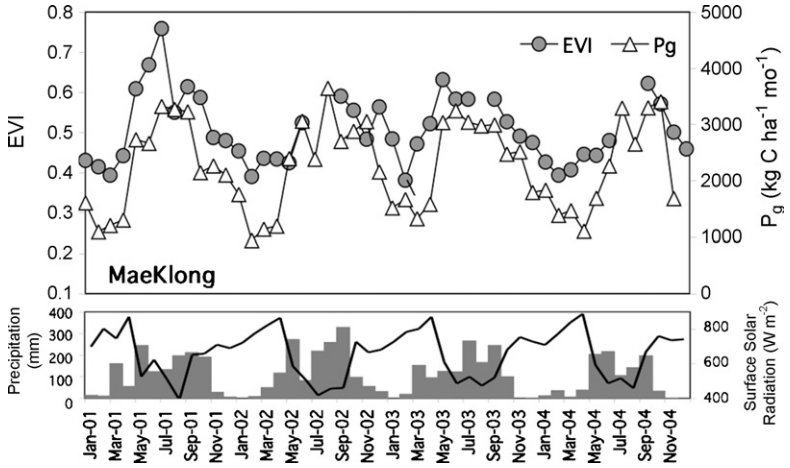

Fig. 2 – Inter-annual and seasonal variations in satellite E_{VI} and tower P_g at MaeKlong Watershed Research Station, Thailand (A) with TRMM-derived precipitation and surface solar radiation measurements (B).

(January–February), resulting in the lowest tower P_g and satellite E_{VI} values in the late dry season (February–April). There was still significant activity in the dry season due to the evergreen species present in this mixed deciduous canopy.

The satellite measure of greenness (E_{VI}) yielded the best overall relationship ($R^2 = 0.88$) with seasonal tower P_g measurements, compared with other MODIS-derived products of P_g, f_{par}, and N_{DVI} (Table 2). The f_{par} product showed very little seasonality while the MODIS P_g product exhibited a seasonal pattern that was partly out of phase with the tower flux measures of P_g (Fig. 3). Satellite E_{VI} and tower flux P_g both showed peak vegetation activity in July. MODIS N_{DVI} was also well correlated with seasonal tower P_g (Table 2).

3.2. *Sakaerat evergreen tropical dry forest*

Seasonal and inter-annual satellite greenness and tower flux P_g measurements were also consistent with each other at the Sakaerat evergreen tropical dry forest site (Fig. 4). As in the MaeKlong drought-deciduous site, these two measures were synchronized with the monsoon rainy period with the lowest values in the late dry season, peak activity in the middle of the wet season, and browning commencing a few months before the rainy season ends. The Sakaerat evergreen site exhibited a weaker seasonality and showed more inter-annual variability, particularly in the late dry season, relative to the MaeKlong site.

MODIS-derived P_g, f_{par}, and N_{DVI} products yielded either very little seasonality or showed seasonal profiles not as well synchronized with tower P_g as the E_{VI} (Table 2; Fig. 5). The strength of the relationship between the independent satellite E_{VI} and tower P_g data remained strong, although somewhat weaker ($R^2 = 0.76$) than at the more deciduous MaeKlong site, and both satellite and tower flux values peaked in August, in contrast to the MaeKlong month of peak activity in July.

Cross-site plots of tower P_g and satellite E_{VI} revealed differences in seasonality at these two tropical dry forest sites, located in fairly similar climate conditions (Fig. 6). The seasonal synchrony across the two sites was generally correlated ($R^2 = 0.47$ for P_g and $R^2 = 0.40$ for E_{VI}), but with slopes that deviated significantly from the 1:1 line, demonstrating the lower seasonality at the Sakaerat evergreen site relative to the MaeKlong drought-deciduous site. During the dry season period in which the lowest P_g and E_{VI} values occur, the Sakaerat evergreen site was more productive than the MaeKlong deciduous site, while during the wet season the MaeKlong deciduous site was the more productive, showing the highest P_g and E_{VI} values. Since the peak E_{VI} and P_g values

Table 2 – Coefficient of determination (R^2, linear model), slope (a), and intercept (b) between seasonal local tower site P_g measurements and MODIS indices, volumetric soil moisture (cm^3/cm^3), surface solar radiation ($W\ m^{-2}$), and $E_{VI} \times I_{par}$ ($W\ m^{-2}$)

	MaeKlong tower P_g			Sakaerat tower P_g			Bukit Soeharto tower P_g			Combined (3 site) tower P_g		
	R^2	a	b	R^2	a	b	R^2	a	b	R^2	a	b
MODIS E_{VI}	**0.88**	7481	−1681	**0.76**	10949	−3727	**0.46**	7123	−1327	**0.74**	8282	−2118
MODIS P_g	**0.07**	−0.55	3453	**0.18**	−0.84	4112	**0.03**	−0.22	3197	**0.00**	−0.09	2594
MODIS f_{par}	**0.01**	−2052	4037	**0.04**	12447	−8550	**0.16**	−3985	5916	**0.05**	−4405	6161
MODIS N_{DVI}	**0.53**	11300	−7018	**0.17**	13467	−9050	**0.00**	419	2323	**0.01**	736	1794
Soil moisture	**0.83**	10412	−1301	**0.32**	18133	175	**0.19**	−3723	3745	**0.08**	1544	1991
Solar radiation	**0.81**	−5.01	5567	**0.48**	−7.51	7665	**0.00**	−0.38	2832	**0.55**	−4.91	5664
$E_{VI} \times I_{par}$	**0.11**	11.75	−80.1	**0.37**	13.52	−974.6	**0.03**	3.43	1962	**0.03**	3.02	1756

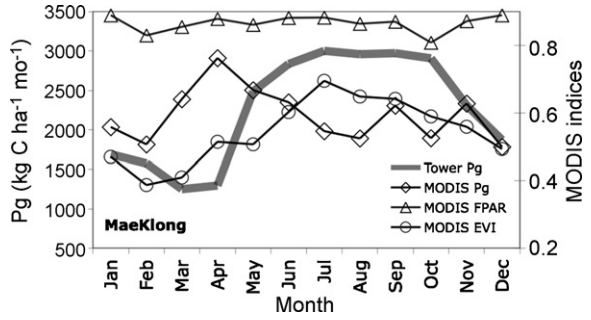

Fig. 3 – Four year averaged seasonal variations in MODIS-derived P_g, f_{par}, and E_{VI} products with averaged tower P_g at MaeKlong Watershed Research Station, Thailand.

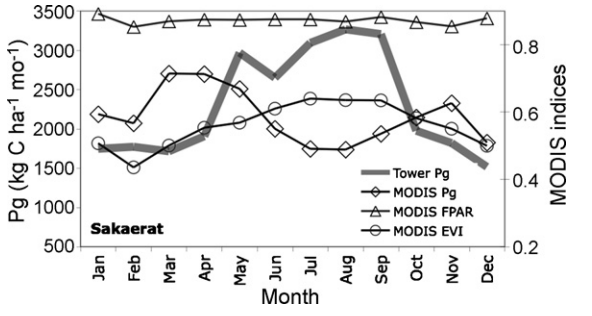

Fig. 5 – Four year averaged seasonal variations in MODIS-derived P_g, f_{par}, and E_{VI} products with averaged tower P_g at Sakaerat Environmental Research Center, Thailand.

between the 2 sites were 1 month apart, we also included a 1-month lagged correlation plot (Fig. 6). The 1-month lagged relationship in the cross-site tower P_g measurements was improved (R^2 from 0.46 to 0.58), however, there was no change in the satellite E_{VI} relationship. In both datasets the slope of the relationships did not significantly change.

3.3. *Bukit Soeharto humid evergreen tropical forest*

Temporal variations in tower P_g and satellite E_{VI} at the Bukit Soeharto humid evergreen rainforest site, showed weak to moderate seasonal differences in greenness and productivity (Fig. 7). This was a particularly difficult site to obtain good quality satellite data due to a lower seasonality and heavy cloud cover conditions. Both inter-annual and annual averaged E_{VI} and tower P_g profiles were generally consistent with both measures revealing peak activity during the dry season months (June–August) (Fig. 8). The relationships of tower P_g with MODIS vegetation products were much weaker, with the E_{VI} yielding the best overall relationship ($R^2 = 0.46$). The seasonal amplitudes in tower P_g and satellite E_{VI} appear to be increasing from 2001 through 2004, suggesting a dynamic and developing secondary forest canopy.

When the 3 tropical forest sites were combined into a single plot, the cross-site tower P_g–satellite E_{VI} relationship accounted for nearly 74% of the variance ($R^2 = 0.74$) (Fig. 9). The local site relationships were not significantly different from the mean, cross-site relationship, however, the evergreen dry forest (driest site) had a slightly steeper slope, while the MaeKlong site had a slope relationship nearly the same as that of the cross-site relationship.

3.4. *Environmental controls on productivity*

The tower P_g measures of vegetation productivity and satellite E_{VI} were positively correlated with soil water status at the MaeKlong and Sakaerat tropical dry forest sites (Fig. 10). The drought-avoiding and more water conserving Sakaerat evergreen forest site had the steepest P_g–soil moisture relationship (Fig. 10). This site, with its coarse textured soil, also had distinctly lower soil moisture levels than the other two sites. The Bukit Soeharto site had the most decoupled P_g relationship with soil moisture content, with a slight negative slope. Tower P_g and satellite E_{VI} relationships with soil moisture were generally consistent with each other at each site, including the negative relationship at the Bukit Soeharto site (Fig. 10).

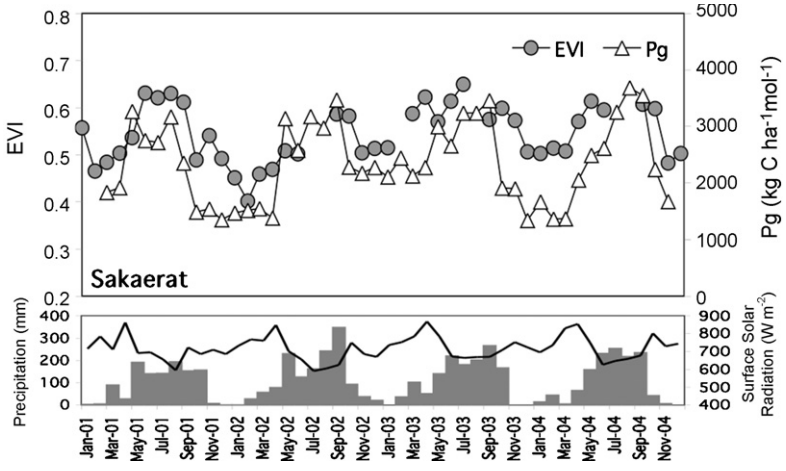

Fig. 4 – Inter-annual and seasonal variations in satellite E_{VI} and tower P_g at Sakaerat Environmental Research Center, Thailand (A) with TRMM-derived precipitation and surface solar radiation measurements (B).

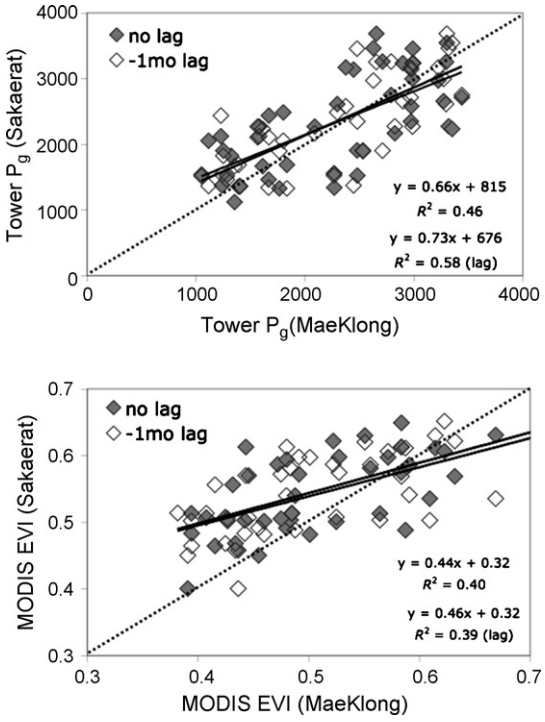

Fig. 6 – Cross-site comparisons of (A) tower P_g and (B) satellite E_{VI} seasonality between two tropical dry forest type sites, MaeKlong drought-deciduous forest and Sakaerat evergreen forest for 1 month lag and no lag cases.

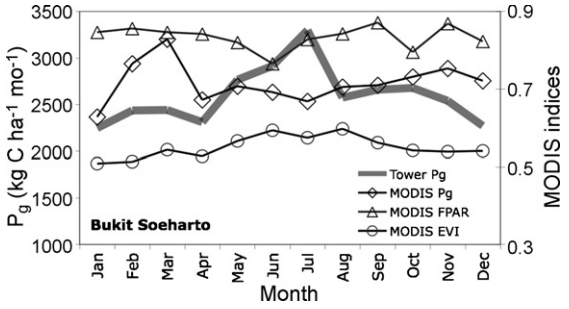

Fig. 8 – Four year averaged seasonal variations in MODIS-derived P_g, f_{par}, and E_{VI} products with averaged tower P_g at Bukit Soeharto Station, Indonesia.

Seasonal tower P_g fluxes yielded negative relationships with seasonal patterns of surface solar radiation (Table 2). The drought-deciduous MaeKlong site had the strongest negative relationship ($R^2 = 0.81$), as higher periods of surface solar radiation occurred in the dry season when P_g was lower, and lower solar radiation occurred in the more cloudy wet season when P_g values were at their highest. The Sakaerat site had a moderately negative relationship with solar radiation and there was no relationship at the Bukit Soeharto site.

In many ecosystem light-use efficiency (LUE) models, the satellite-derived vegetation index is normally used as a canopy state variable of photosynthesis potential or capacity, according to,

$$P_g = \varepsilon f_{par} I_{par} \quad (3)$$

$$f_{par} = aV_I + b \quad (4)$$

where ε is the LUE, f_{par} is the fraction of I_{par} absorbed by the canopy, and V_I is the vegetation index (normally N_{DVI}), which is generally considered to be linear (slope a and intercept b) with f_{par} (Ruimy et al., 1999; Sims et al., 2006; Jenkins et al., 2007). Whereas, the N_{DVI} has been shown linearly related with canopy f_{par}, Xiao et al. (2004) distinguished between the photosynthetically active and non-photosynthetically active components of canopy absorbed radiation and reported the E_{VI} to be more closely related to the chlorophyll component of f_{par}. We analyzed whether the inclusion of I_{par} data, as $E_{VI} \times I_{par}$, could improve upon the direct relationship of P_g with E_{VI},

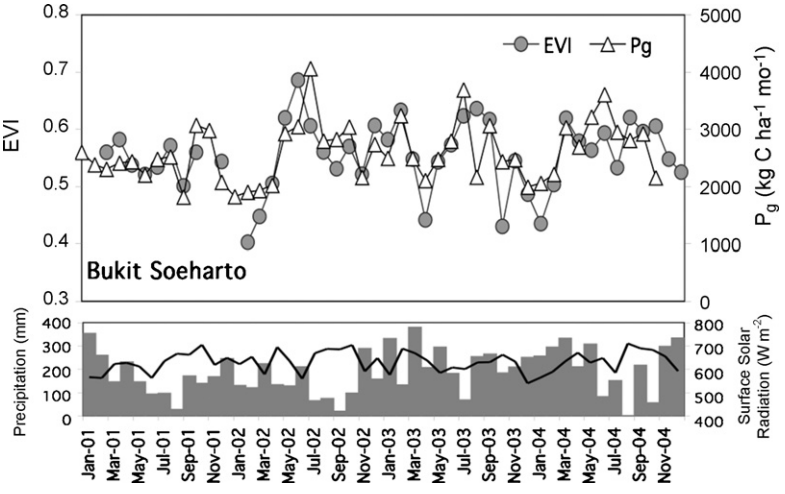

Fig. 7 – Inter-annual and seasonal variations in satellite E_{VI} and tower P_g at Bukit Soeharto Station, Indonesia (A) with TRMM-derived precipitation and surface solar radiation measurements (B).

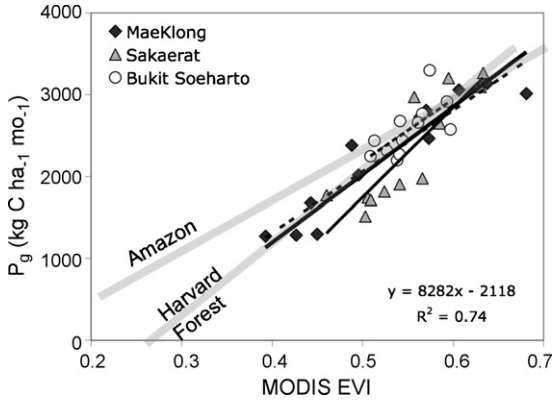

Fig. 9 – Combined multiple site annual averaged relationships between tower P_g and satellite E_{VI}. The shaded lines refer to equivalent relationships encountered in the Amazon (rainforest + pasture) and Harvard Forest (temperate forest) sites.

however, no site specific nor cross-site improvements were found (Table 2).

3.5. *Phenoregion analyses for regional extension*

A phenoregion perspective of seasonal vegetation dynamics was depicted by the month of annual peak in E_{VI} greenness activity for each 1 km^2 pixel (Fig. 1). The two Thailand tropical dry forest tower sites are located in upland mountain areas with greenness peaks in the middle of the rainy wet season, in July and August. These sites are surrounded by highly heterogeneous phenology patterns with large differences in greenness seasonality, related to topography, climate, land use, soils, and vegetation type. Whereas the 2 tower sites are located at elevations of 160 and 535 m, the surrounding higher elevation sites (>1000 m) experience peak greenness activity in the late dry season and early wet season (May), i.e., the 'green' colors near Sakaerat and MaeKlong sites and eastern Myanmar. This suggests that higher elevation, montane tropical forests may be light-limited, as in the forests of northern Thailand that were found with transpiration peaks in the late dry season (Tanaka et al., 2003, 2004).

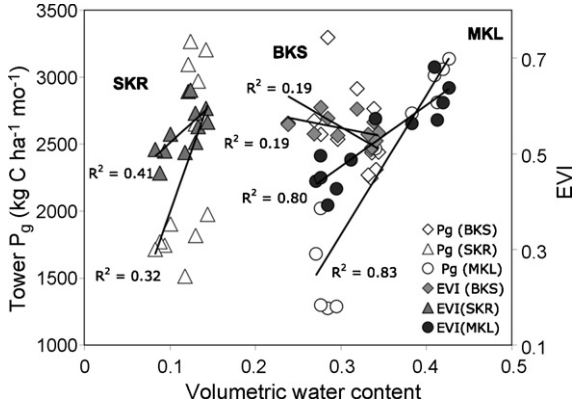

Fig. 10 – Tower P_g (A) and MODIS E_{VI} (B) relationships with volumetric soil moisture contents (cm^3/cm^3) at 10 cm depth across the three tropical forest sites; MKL = MaeKlong; SKR = Sakaerat; and BKS = Bukit Soeharto.

The drier northeast region of Thailand, which is mostly cultivated with remnants of deciduous forest, shows peak satellite greenness activity at the end of the rainy season and start of the dry season (November–December). Once soil moisture levels deplete, this area rapidly dries out. The central region that follows the Chao Praya River is dominated by irrigated crops and riparian vegetation that is not moisture stressed and with peak greenness activity in February, the middle of the dry season. The large heterogeneity within each subregion may be depicting a variety of land use activities and human impacted areas, as well as forests at various stages of regeneration.

By contrast the equatorial region shows a distinctly different pattern of satellite phenology activity, dominated by 'blue' colors, indicative of peak activity in February and March, the middle of the wet season at this latitude (Figs. 1 and 7). The region-wide predominant phenology observed, synchronous with the rainy season, suggests that most of this area becomes water-limited during the short dry season. Thus, extensive forest disturbance and degradation, through fire and logging activities, have resulted in most of this region, including Kalimantan, being transformed to a water-limited system, despite its abundant rainfall. There are many distinctive 'yellow' areas of peak greenness activity that occur in the dry season (July), including the protected Bukit Soeharto site. The mountainous region between Malaysia and Kalimantan also has some protected areas with intact forests, which show peak greenness activity at the end of the dry season and beginning of the wet season (October–November, 'purple colors'), suggesting that this remote region may also exhibit light limitations.

To depict seasonal P_g variations over the tropical Monsoon Asia region, we applied the general relationship of tower P_g with satellite E_{VI}, as in Fig. 9, over a wet and dry season period (Fig. 11). The uncertainty in predicting P_g from only satellite E_{VI} data is approximately 300 kg C ha^{-1} mo^{-1} based on the range of seasonal P_g values encountered across the 3 sites of this study. In the January–March period, it is the dry season in the northern portion of the region (Lat. 10 to 20°N) and wet season in the southern portion (Lat. 5 N to 5°S). In the northern part, the forested areas have P_g values of 2000 kg C ha^{-1} mo^{-1}, while the deforested northeast plateau of Thailand and other cultivated areas of the region have P_g values from 0 to 1000 kg C ha^{-1} mo^{-1} (Fig. 11a). In contrast, the southern region has higher P_g values ranging from 2000 to 3500 kg C ha^{-1} mo^{-1}.

In the June to August period, it is the wet season in the northern region and dry season to the south (Fig. 11b). The region-wide shift to higher P_g values in the north is readily apparent. The southern region maintains high P_g values in both wet and dry periods, with slightly lower values occurring in the dry season. This does not match the results from the tower site and satellite data within the protected Bukit Soeharto area, in which higher P_g and E_{VI} were encountered in the dry season period. As in the northern tower sites, such protected areas do not adequately represent the range of land surface conditions of Southeast Asia, particularly the extensive areas of disturbed, degraded, and unprotected forests.

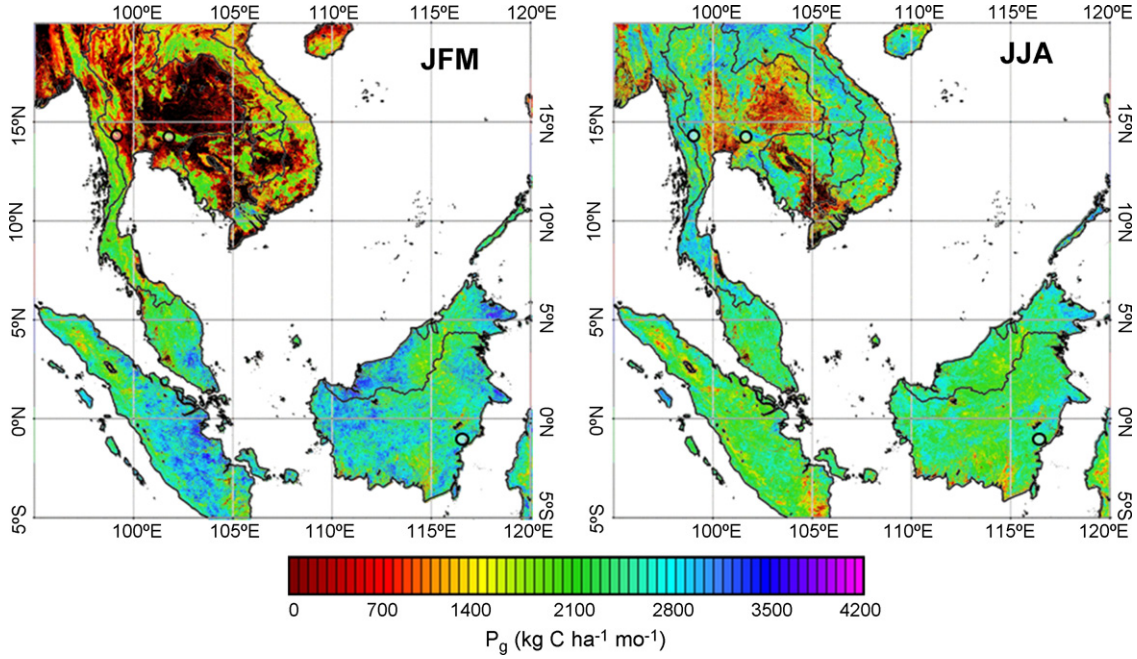

Fig. 11 – Region-wide satellite E_{VI}-derived P_g using general site tower relationship for January to March (JFM) and June to August (JJA) periods.

4. Discussion and conclusions

In this study, we found significant phenologic variability across three different tropical forest types, encompassing evergreen and deciduous canopies over varying climate, soil, and disturbance conditions. Distinct tropical forest responses to seasonal drought periods were observed across all forest types, including drought-avoiding (MaeKlong dry deciduous site), drought-tolerant (Sakaerat dry evergreen site), and enhanced productivity (Bukit Soeharto humid evergreen site) responses. Independent satellite E_{VI} greenness measurements were generally consistent with the seasonal and inter-annual patterns observed in the *in situ* tower P_g measurements.

Seasonal tower P_g and satellite greenness measurements in the dry evergreen (Sakaerat) and drought-deciduous (MaeKlong) forests showed photosynthetic activity tightly coupled with soil water availability and precipitation seasonality. Both satellite greenness and tower P_g fluxes showed the dry evergreen tropical forest to have less pronounced seasonality, higher productivity in the dry season, and lower productivity in the wet season, relative to the more drought-deciduous forest site. As noted by Sobrado (1993), the shorter lived leaves of the drought-avoiding deciduous species were capable of high carbon gain during the short, wet season in nutrient-rich soils, while the long-lived leaves of the drought-tolerant evergreen species were capable of low carbon gain and conservative water-use over both the wet and dry seasons in nutrient-poor soils.

The more humid evergreen rainforest site in Indonesia (Bukit Soeharto), showed the weakest tower P_g–MODIS E_{VI} relationship ($R^2 = 0.46$), with tower P_g and satellite greenness temporal patterns that were largely decoupled from seasonal variations in moisture. The protected Bukit Soeharto humid evergreen rainforest site was more productive in the middle of the dry season than in the wet season, despite being a relatively young, regenerating forest that was completely burned in the 1997–1998 El Niño event. This suggests some degree of drought-tolerance and light-limitations in these young forests and that the more mature and deep-rooted rainforests of this region would be more drought-tolerant and light-limited. However, as seen in the satellite-derived regional P_g estimates (Fig. 11), most of the island of Borneo appeared moisture-limited rather than light-limited as found in the protected Bukit Soeharto site. Large scale and frequent fires and forest degradation have dramatically altered the productivity and phenology controls of the mostly secondary forests of Borneo and rendered these areas vulnerable to moisture limitations, primarily in the shallow-rooted, understorey herbaceous vegetation layer, and also in the trees themselves, depending on their age class and stage of root development (Curran et al., 2004).

The satellite E_{VI} greenness measure behaved linearly with tower P_g across the multiple Monsoon Asia tower sites and range of ecosystems studied here. The tower P_g relationships with MODIS E_{VI} were also generally consistent with the relationships found in the Amazon rainforest and temperate forests (shown in Fig. 9 with shaded lines), with tower $P_g = 6418E_{VI} - 800$($R^2 = 0.54$) at two Amazon tower sites (km 67, primary forest and km 77, pasture-agriculture site) and tower $P_g = 8488E_{VI} - 2223$($R^2 = 0.79$) at the Harvard Forest temperate site, with units kg C ha^{-1} mo^{-1} (Sims et al., 2006; Rahman et al., 2005; Huete et al., 2006).

Despite the general consistencies encountered, there were significant differences in the slopes of the tower P_g with satellite E_{VI} relationships. Rahman et al. (2005) and Sims et al. (2006) further noted that MODIS E_{VI} was less strongly correlated with tower P_g over evergreen sites in North America that displayed less seasonality than their deciduous ecosys-

tem counterparts that often go dormant in their cold winter seasons. Our results similarly showed weaker tower P_g and satellite greenness relationships with the more evergreen canopies, however, the relationships encountered were quite strong, given the lack of a cold or dormant season in the tropical forests studied here.

Satellite greenness observations and tower flux measurements represent important site-specific and landscape-level responses to environmental variation and change. The eddy flux measures are limited in spatial extent, but collect data at high temporal resolution, while satellite measurements are extensive and integrate numerous spatial heterogeneities in vegetation types, soil, topography, and disturbance condition, however, they are constrained temporally, primarily due to clouds. In this study, we found seasonal consistencies between independent satellite E_{VI} and *in situ* tower P_g relationships at all sites, as well as in their respective relationships to environmental controls, such as soil moisture and solar radiation (Figs. 2, 4, 7 and 10). These consistencies lend confidence to both datasets and offer opportunities for more extensive regional scaling of tower fluxes with satellite data. However, there remain many challenges on how best to integrate spatially extensive satellite data with local tower measures from multiple sites for regional scaling, modeling, and prediction of vegetation growth in response to climate variability across Monsoon Asia.

High temporal frequency, moderate resolution satellite data, such as MODIS, are critical to achieve greater sensitivity to phenological variations, however, such data may be too coarse, spatially, to adequately define the highly heterogenous landscapes in Monsoon Asia, associated with disturbance, land-use classes, and forest fragmentation patterns (Fig. 1). Furthermore, as in this study, cloud cover greatly restricted the availability of good quality satellite data to monthly resolutions in the more humid tropical areas.

Further work is also needed on how best to integrate satellite data into ecosystem production efficiency models (Eqs. (3) and (4)). There were difficulties in coupling tower flux measurements with the MODIS P_g product due to the additional uncertainties associated with coarser and less accurate satellite meteorological variables and MODIS f_{par}, which exhibited very little seasonality at all three sites. Our attempt to improve upon the satellite E_{VI} and tower P_g relationship through the use I_{par} was also unsuccessful. As suggested by Xiao et al. (2004, 2005), there is a need to better separate I_{par} absorbed by a canopy into the photosynthetically active (chlorophyll) and non-active (senesced vegetation, woody material, etc.) components. Jenkins et al. (2007) observed a linear relationship between N_{DVI} and f_{par} during greening and a non-linear relationship during seasonal drying periods, a hysteresis effect that may complicate the remote sensing use of ecosystem production efficiency models.

As a result of the more complex environments (topography, soils, land use) in Monsoon Asia tropical forests, relative to the Amazon, our results are not entirely conclusive as to whether neotropical and Monsoon Asia tropical ecosystems respond similarly to light and rainfall controls. Moisture limitations on the productivity of tropical dry forests in Thailand are consistent with other studies in the southern, transitional forests of the Amazon (e.g., Vourlitis et al., 2001) and in the tropical dry forests of Mexico and Central America (e.g., Reich and Borchert, 1984). We found some indication of light limitations at the Indonesia humid evergreen secondary forest tower site, with peak tower P_g and E_{VI} values in the dry season. As revealed by regional satellite phenology data and satellite-derived P_g images, this protected site is surrounded by degraded coastal lowland secondary forests exhibiting moisture-limiting phenologies (Figs. 1 and 11). The three tower sites analyzed here were largely confined to three forest types located in protected areas, and thus represent a very restrictive range of land surface conditions found in this region. Eddy flux tower comparisons with satellite data are needed over a greater range of land surface conditions, particularly areas of disturbed, degraded, and unprotected forests, for more effective coupling of satellite and tower data for regional scaling studies of ecosystem function and carbon and water cycling.

Acknowledgements

We greatly thank the Oak Ridge National Laboratory Distributed Active Archive Center (ORNL DAAC) for the availability of MODIS subsetted land products, Collection 5, for all three flux tower sites [http://www.daac.ornl.gov/MODIS/modis.html]. This study was supported by NASA MODIS contract NNG04HZ20C.

REFERENCES

Achard, F., Estreguil, C., 1995. Forest classification of southeast Asia using NOAA AVHRR data. Remote Sensing of Environment 54 (3), 198–208.

Achard, F., Eva, H.D., Stibig, H.-J, Mayaux, P., Gallego, J., Richards, T., Malingreau, J.-P., 2002. Determination of deforestation rates of the world's humid tropical forests. Science 297 (0036–8075), 999–1002.

Asner, G.P., Nepstad, D., Cardinot, G., Ray, D., 2004. Drought stress and carbon uptake in an Amazon forest measured with spaceborne imaging spectroscopy. Proceedings of the National Academy of Science 101 (16), 6039–6044.

Canadell, J., Jackson, R.B., Ehleringer, J.B., Mooney, H.A., Sala, O.E., Schulze, E.-D., 1996. Maximum rooting depth of vegetation types at the global scale. Oecologia 108 (4), 583–595.

Carswell, F.E., Costa, A.L., Palheta, M., Mahli, Y., Meir, P., Costa, J. de P.R., Ruivo, M. de L., Leal, L.do S.M., Costa, J.M.N., Clement, R.J., Grace, J., 2002. Seasonality in CO_2 and H_2O flux at an eastern Amazonian rain forest. Journal of Geophysical Research 107 (D 20), 8076.

Cihlar, J., Hung, L., Zhanqing, L., Jing, C., Pokrant, H., Fengting, H., 1997. Multitemporal, multichannel AVHRR data sets for land biosphere studies—artifacts and corrections. Remote Sensing of Environment 60 (1), 35–57.

Curran, L.M., Trigg, S.N., McDonald, A.K., Astiani, D., Hardiono, Y.M., Siregar, P., Caniago, I., Kasischke, E., 2004. Lowland forest loss in protected areas of Indonesian Borneo. Science 303 (5660), 1000–1003, doi:10.1126/science.1091714.

da Rocha, H.R., Goulden, M.L., Miller, S.D., Menton, M.C., Pinto, L.D.V.O., de Freitas, H.C., Figueira, A.M.S., 2004. Seasonality of water and heat fluxes over a tropical forest in eastern Amazonia. Ecological Applications 14 (4), S22–S32.

Defries, R.S., Field, C.B., Fung, I., Justice, C.O., Los, S., Matson, P.A., Matthews, E., Mooney, H.A., Potter, C.S., Prentice, K., Sellers, P.J., Townshend, J.R.G., Tucker, C.J., Ustin, S.L., Vitousek, P.M., 1995. Mapping the land surface for global atmosphere-biosphere models—toward continuous distributions of vegetations functional properties. Journal of Geophysical Research-Atmospheres 100 (D 10), 20867–20882.

Eva, H.D., Belward, A.S., de Miranda, E.E., Bella, C.M.D., Gond, V., Huber, O., Jones, S., Sgrenzaroli, M., Fritz, S., 2004. A land cover map of South America. Global Change Biology 10, 731–744.

Gamo, M., Panuthai, S., Maeda, T., Toma, T., Ishida, A., Hayashi, M., Warsudi, Dianna, R., Diloksumpun, S., Phanumard, L., Staporn, D., Ishizuka, M., Saigusa, N., Kondo, H., 2005. Carbon flux observation in the tropical seasonal forests and tropical rain forest. In: Proceedings of the International Workshop on Advanced Flux Network and Flux Evaluation (AsiaFlux Workshop 2005), Fujiyoshida, Japan, p. 86.

Frankie, G.W., Baker, H.G., Opler, P.A., 1974. Comparative phenological studies of trees in tropical wet and dry forests in the lowlands of Costa Rica. The Journal of Ecology 62 (3), 881–919.

Goulden, M.L., Munger, J.W., Fan, S.-M., Daube, B.C., Wofsy, S.C., 1996. Measurements of carbon sequestration by long-term eddy covariance: methods and a critical evaluation of accuracy. Global Change Biology 2, 169–182.

Goulden, M.L., Miller, S.D., da Rocha, H.R., Menton, M.C., de Freitas, H.C., Figueira, A.M.S., Sousa, C.A.D.de., 2004. Diel and seasonal patterns of tropical forest CO_2 exchange. Ecological Applications 14, S42–S54.

Goward, S.N., Markham, B., Dye, D.G., Dulaney, W., Yang, J., 1991. Normalized difference vegetation index measurements from the advanced very high resolution radiometer. Remote Sensing of Environment 35 (2–3), 257–277.

Huete, A., Didan, K., Miura, T., Rodriguez, E.P., Gao, X., Ferreira, L.G., 2002. Overview of the radiometric and biophysical performance of the MODIS vegetation indices. Remote Sensing of Environment 83 (1–2), 195.

Huete, A.R., K.D., Shimabukuro, Y.E., Ratana, P., Saleska, S.R., Hutyra, L.R., Yang, W., Nemani, R.R., Myneni, R., 2006. Amazon rainforests green-up with sunlight in dry season. Geophysical Research Letters, 33(L06405): doi:10.1029/2005GL025583.

Huete, A.R., Kim, Y., Ratana, P., Didan, K., Shimabukuro, Y.E., Miura, T., 2008. Assessment of phenologic variability in Amazon tropical rainforests using hyperspectral Hyperion and MODIS satellite data. In: Kalacska, M., Sanchez-Azofeifa, A.G. (Eds.), Hyperspectral Remote Sensing of Tropical and Sub-Tropical Forests. Taylor & Francis Group, LLC, CRC Press, 352 pp.

Hutyra, L.R., Munger, J.W., Saleska, S.R., Gottlieb, E., Daube, B.C., Dunn, A.L., Amaral, D.F., de Camargo, P.B., Wofsy, S.C., 2007. Seasonal controls on the exchange of carbon and water in an Amazonian rain forest. Journal of Geophysical Research, Biogeosciences 112 (G3) Art. No. G03008.

Ishida, A., Diloksumpun, S., Ladpala, P., Staporn, D., Panuthai, S., Gamo, M., Yazaki, K., Ishizuka, M., Puangchit, L., 2006. Contrasting seasonal leaf habits of canopy trees between tropical dry-deciduous and evergreen forests in Thailand. Tree Physiology 26 (5), 643–656.

Jenkins, J.P., Richardson, A.D., Braswell, B.H., Ollinger, S.V., Hollinger, D.Y., Smith, M.-L., 2007. Refining light-use efficiency calculations for a deciduous forest canopy using simultaneous tower-based carbon flux and radiometric measurements. Agricultural and Forest Meteorology 143 (1–2), 64–79.

Justice, C., Hall, D., Salomonson, V.V., Privette, J., Riggs, G., Strahler, A., Lucht, W., Myneni, R., Knjazihhin, Y., Running, S., Nemani, R., Vermote, E., Townshend, J., Defries, R., Roy, D., Wan, Z., Huete, A., van Leeuwen, W., Wolfe, R., Giglio, L., Muller, J.-P., Lewis, P., Barnsley, M., 1998. The Moderate Resolution Imaging Spectroradiometer (MODIS): Land remote sensing for global change research. IEEE Transactions on Geoscience and Remote Sensing 36, 1228–1249.

Justice, C.O., Townshend, J.R.G., Holben, B.N., Tucker, C.J., 1985. Analysis of the phenology of global vegetation using meteorological satellite data. International Journal of Remote Sensing 6 (8), 1271–1318.

Kalacska, M.E.R., Sánchez-Azofeifa, G.A., Calvo-Alvarado, J.C., Rivard, B., Quesada, M., 2005. Effects of season and successional stage on leaf area index and spectral vegetation indices in three Mesoamerican tropical dry forests. Biotropica 37 (4), 486–496.

Keller, M., Alencar, A., Asner, G.P., Braswell, B., Bustamante, M., Davidson, E., Feldpausch, T., Fernandes, E., Goulden, M., Kabat, P., Kruijt, B., Luizao, F., Miller, S., Markewitz, D., Nobre, A.D., Nobre, C.A., Filho, N.P., da Rocha, H., Dias, P.S., von Randow, C., Vourlitis, G.L., 2004. Ecological research in the large-scale biosphere-atmosphere experiment in Amazonia: early results. Ecological Applications 14 (4), S3–S16.

Kobayashi, H., Dye, D.G., 2005. Atmospheric conditions for monitoring the long-term vegetation dynamics in the Amazon using normalized difference vegetation index. Remote Sensing of Environment 97 (4), 519–525.

Kushwaha, C.P., Singh, K.P., 2005. Diversity of leaf phenology in a tropical deciduous forest in India. Journal of Tropical Ecology 21 (1), 47–56.

Lean, J., Rowntree, P.R., 1993. A GCM simulation of the impact of Amazonian deforestation on climate using an improved canopy representation. Quarterly Journal of the Royal Meteorological Society 119 (511), 509–530.

Mahli, Y., Nobre, A.D., Grace, J., Kruijt, B., Pereira, M.G.P., Culf, A., Scott, S., 1998. Carbon dioxide transfer over a Central Amazonian rain forest. Journal of Geophysical Research 103 (D24), 31,593–31,612.

Mayaux, P., Lambin, E.F., 1997. Tropical forest area measured from global land-cover classifications: inverse calibration models based on spatial textures. Remote Sensing of Environment 59 (1), 29–43.

Myneni, R.B., Yang, W., Nemani, R.R., Huete, A.R., Dickinson, R.E., Knyazikhin, Y., Didan, K., Fu, R., N.J., R.I., Saatchi, S.S., Hashimoto, H., Ichii, K., Shabanov, N.V., Tan, B., Ratana, P., Privette, J.L., Morisette, J.T., Vermote, E.F., Roy, D.P., Wolfe, R.E., Friedl, M.A., Running, S.W., Votava, P., El-Saleous, N., Devadiga, S., Su, Y., Salomonson, V.V., 2007. Large seasonal swings in leaf area of Amazon rainforests. Proceedings of the National Academy of Science, U.S.A, 20(104(12)): 4820–4823.

NASA, 2007. 3B43: Monthly $0.25^\circ \times 0.25^\circ$ TRMM and other sources rainfall, http://disc.sci.gsfc.nasa.gov/services/opendap/trmm.shtml, NASA Distrib. Active Arch. Cent., Goddard Space Flight Cent. Earth Sci., Greenbelt, Md.

Nemani, R.R., Keeling, C.D., Hashimoto, H., Jolly, W.M., Piper, S.C., Tucker, C.J., Myneni, R., Running, S.W., 2003. Climate-driven increases in global terrestrial net primary production from 1992 to 1999. Science 300, 1560–1563.

Nepstad, D.C., Carvalho, C.R., Davidson, E.A., Jipp, P.H., Lefebvre, P.A., Negreiros, G.H., Silva, E.D., Stone, T.A., Trumbore, S.E., Vieira, S., 1994. The role of deep roots in the hydrological and carbon cycles of Amazonian forests and pastures. Nature 372, 666–669.

Page, S.E., Siegert, F., Rieley, J.O., Boehm, H.D., Jaya, A., Limin, S., 2002. The amount of carbon released from peat and forest fires in Indonesia during 1997. Nature 420 (6911), 29–30.

Pitman, J.I., 1996. Ecophysiology of tropical dry evergreen forest, Thailand: measured and modelled stomatal conductance of

Hopea ferrea, a dominant canopy emergent. Journal of Applied Ecology 33, 1366–1378.
Prior, L.D., Bowman, D.M.J.S., Eamus, D., 2004. Seasonal differences in leaf attributes in Australian tropical tree species: family and habitat comparisons. Functional Ecology 18 (5), 707–718.
Rahman, A.F., Sims, D.A., Cordova, V.D., El-Masri, B.Z., 2005. Potential of MODIS EVI and surface temperature for directly estimating per-pixel ecosystem C fluxes. Geophysical Research Letters 32 (L19404), doi:10.1029/2005GL024127.
Reich, P.B., Borchert, R., 1984. Water stress and tree phenology in a tropical dry forest in the lowlands of Costa Rica. Journal of Ecology 72, 61–74.
Reich, P.B., Uhl, C., Walters, M.B., Prugh, L., Ellsworth, D.S., 2004. Leaf demography and phenology in Amazonian rain forest: A census of 40,000 leaves of 23 tree species. Ecological Monographs 74 (1), 3–23.
Roberts, D.A., Nelson, B.W., Adams, J.B., Palmer, F., 1998. Spectral changes with leaf aging in Amazon caatinga. Trees-Structure and Function 12, 315–325.
Ruimy, A., Kergoat, L., Bondeau, A., Intercomparison, T.P.O.F.T.P.N.M., 1999. Comparing global models of terrestrial net primary productivity (NPP): analysis of differences in light absorption and light-use efficiency. Global Change Biology 5, 56–64.
Rundel, P.W., Boonpragob, K., 1995. Dry forest ecosystems of Thailand. In: Bullock, S.H., Mooney, H.A., Medina, E. (Eds.), Seasonally Dry Tropical Forests. Cambridge University Press, Cambridge, pp. 93–123.
Running, S.W., Justice, C., Salomonson, V.V., Hall, D., Barker, J., Kaufman, Y., Strahler, A., Huete, A., Muller, J.P., Vanderbilt, V., Wan, Z.M., Teillet, P., Carneggie, D., 1994. Terrestrial remote sensing science and algorithms planned for EOS/MODIS. International Journal of Remote Sensing 15, 3587–3620.
Sader, S.A., Waide, R.B., Lawrence, W.T., Joyce, A.T., 1989. Tropical forest biomass and successional age class relationships to a vegetation index derived from Landsat TM data. Remote Sensing of Environment 28, 143–156.
Saleska, S.R., Didan, K., Huete, A.R., da Rocha, H.R., 2007. Amazon forests green-up during 2005 drought. Science 318, 612.
Saleska, S.R., Miller, S.D., Matross, D.M., Goulden, M.L., Wofsy, S.C., da Rocha, H.R., de Camargo, P.B., Crill, P., Daube, B.C., de Freitas, H.C., Hutyra, L., Keller, M., Kirchhoff, V., Menton, M., Munger, J.W., Pyle, E.H., Rice, A.H., Silva, H., 2003. Carbon in Amazon forests: unexpected seasonal fluxes and disturbance-induced losses. Science 302, 1554–1557.
Schurr, U., Walter, A., Rascher, U., 2006. Functional dynamics of plant growth and photosynthesis - from steady-state to dynamics - from homogeneity to heterogeneity. Plant, Cell & Environment 29, 340–352.
Meeson, B.W., Hall, F.G., Asrar, G., Murphy, R.E., Schiffer, R.A., Bretherton, F.P., Dickinson, R.E., Ellingson, R.G., Field, C.B., Huemmrich, K.F., Justice, C.O., Melack, J.M., Roulet, N.T., Schimel, D.S., Try, P.D., Sellers, P.J., 1995. Remote sensing of the land surface for studies of global change: models–algorithms–experiments. Remote Sensing of Environment 51 (1), 3–26.
Shuttleworth, W.J., 1988. Evaporation from Amazonian Rainforest. Proceedings of the Royal Society of London. Series B, Biological Sciences, 233 (1272) 321–346.
Sims, D.A., Rahman, A.F., Cordova, V.D., El-Masri, B.Z., Baldocchi, D.D., Flanagan, L.B., Goldstein, A.H., Hollinger, D.Y., Misson, L., Monson, R.K., Oechel, W.C., Schmid, H.P., Wofsy, S.C., Xu, L., 2006. On the use of MODIS EVI to assess gross primary productivity of North American ecosystems, Journal of Geophysical Research, 111, G04015, doi:10.1029/2006JG000162.
Skole, D., Tucker, C., 1993. Tropical deforestation and habitat fragmentation in the Amazon, Satellite data from 1978 to 1988. Science 260, 1905–1910.
Skole, D.L., Qi, J., 2001, Optical remote sensing for monitoring forest and biomass change in the context of the Kyoto Protocol, CGCEO/RA01-01/w. Michigan State University, East Lansing, Michigan.
Sobrado, M.A., 1993. Trade-off between water transport efficiency and leaf life-span in a tropical dry forest. Oecologia 96 (1), 19–23.
Tanaka, K., Takizawa, H., Kume, T., Xu, J., Tantasirin, C., Suzuki, M., 2004. Impact of rooting depth and soil hydraulic properties on the transpiration peak of an evergreen forest in northern Thailand in the late dry season, Journal of Geophysical Research, 109, D23107, doi:10.1029/2004JD004865.
Tanaka, K., Takizawa, H., Tanaka, N., Kosaka, I., Yoshifuji, N., Tantasirin, C., Piman, S., Suzuki, M., Tangtham, N., 2003. Transpiration peak over a hill evergreen forest in northern Thailand in the late dry season: Assessing the seasonal changes in evapotranspiration using a multilayer model. Journal of Geophysical Research 108 (D17), 4533, doi:10.1029/2002JD003028.
Tian, H., Melillo, J.M., Kicklighter, D.W., Pan, S., Liu, J., McGuire, A.D., Moore III, B., 2003. Regional carbon dynamics in monsoon Asia and its implications for the global carbon cycle. Global and Planetary Change 37 (3–4), 201–217.
Vieira, I.C., Almeida, A.S., Davidson, E.A., Stone, T.A., Carvalho, C.J.R., Guerrero, J.B., 2003. Classifying successional forest stages using Landsat spectral properties and ecological characteristics in eastern Amazonia. Remote Sensing of Environment 87, 470–481.
Viña, A., Henebry, G.M., 2005. Spatio-temporal change analysis to identify anomalous variation in the vegetated land surface: ENSO effects in tropical South America. Geophysical Research Letters 32 (21), 1–5.
Vourlitis, G.L., Filho, N.P., Hayashi, M.M.S., Nogueira, J. De S., Caseiro, F.T., Campelo Jr., J.H., 2001. Seasonal variations in the net ecosystem CO_2 exchange of a mature Amazonian transitional tropical forest (cerradão). Functional Ecology 15, 388–395.
White, M.A., Hoffman, F., Hargrove, W.W., Nemani, R.R., 2005. A global framework for monitoring phenological responses to climate change, Geophysical Research Letters, 32, L04705, doi:10.1029/2004GL021961.
Wright, S.J., Schaik, C.P., 1994. Light and the phenology of tropical trees. American Naturalist 143, 192–199.
Xiao, X., Hagen, S., Zhang, Q., Keller, M., Moore Iii, B., 2006. Detecting leaf phenology of seasonally moist tropical forests in South America with multi-temporal MODIS images. Remote Sensing of Environment 103 (4), 465–473.
Xiao, X., Zhang, Q., Braswell, B., Urbanski, S., Boles, S., Wofsy, S., Moore, B., Ojima, D., 2004. Modeling gross primary production of temperate deciduous broadleaf forest using satellite images and climate data. Remote Sensing of Environment 91, 256–270.
Xiao, X., Zhang, Q., Saleska, S., Hutyra, L., De Camargo, P., Wofsy, S., Frolking, S., Boles, S., Keller, M., Moore III, B., 2005. Satellite-based modeling of gross primary production in a sesonally moist tropical evergreen forest. Remote Sensing of Environment 94 (1), 105–122.
Zhang, Q., Xiao, X., Braswell, B., Linder, E., Baret, F., Moore III, B., 2005. Estimating light absorption by chlorophyll, leaf and canopy in a deciduous broadleaf forest using MODIS data and a radiative transfer model. Remote Sensing of Environment 99 (3), 357.